JOURNAL INDIAN ASSOCIATION OF SEDIMENTOLOGISTS ISSN NO 2582 – 2020
Vol. 41, Issue II, 2024, pp. 40 – 51
DOI: https://doi.org/10.51710/jias.v41iII.382

Morphometric evaluation of diverse ripple structures in the Alwar Group at Jamwa Ramgarh in NE Rajasthan, North Delhi Fold Belt, NW India

Asha Saxena*, M. K. Pandit, Nirmal Kant Verma
Department of Geology, University of Rajasthan, Jaipur-302004 (India)
* E-mail Address: ashageo19@gmail.com
***** ORCID: 0000-0002-7983-3034

ABSTRACT

In this study we describe a complex set of well-preserved ripple structures from the Alwar Group quartzites (quartz arenite) of Mesoproterozoic Delhi Supergroup in NW India. Exposed in a road section near Jamwa Ramarh (to the east of Jaipur city), a large abundance and diversity in ripple shape, size, wave amplitude and mode of occurrence is unique for a small geographic area. The studied ripples are predominantly symmetric in shape, showing bifurcations, sinuous types, pointed crest with rounded trough, etc. Occasional current and criss-cross, and mega ripples are also present. Their symmetric shape suggests a wave dominant environment. The Vertical Form Index (VFI) values or Ripple Index values below 15 further rule out any possibility of a wind origin for them. The criss-cross and interference ripples point toward the presence of a high energy river system in the vicinity. The statistical analysis of ripple morphological parameters indicates deposition of quartz arenite under shallow water conditions (< 3 m depth). Based on various morphometric analyses, we infer continental shelf with variable depth for the development of these wave ripples. Based on the crest-line criterion, the inferred paleocurrent direction was from the NW.

Keywords: Ripples, classification, morphometric analysis, quartz arenite, Alwar Group, NW India

INTRODUCTION

One of the primary objectives of a sedimentological investigation is to reconstruct the depositional environment and infer the paleocurrent direction. While heavy minerals are reliable tools in source characterization, the primary sedimentary structures are the diagnostic indicators of paleo-sedimentary depositional processes. Ripple marks (also named, ripples, current marks, wave marks, and friction marks), are one of the most common primary structures preserved in the arenaceous (arenite) rocks (Tanner, 1982). Formed by non-cohesive materials under the action of water, waves or wind, the ripple marks are one of the most prevalent sedimentary structures and are regarded as significant indicators of the near-shore, fluvial and aeolian depositional environment. Different aspects of ripple morphology are commonly investigated, such as the shape, classification (Baird, 1962), formation and evolution (Bergman, 1979, Chang and Fleming, 2013) etc. that are useful in sedimentary environment modelling and paleoclimate reconstruction (De Vleeschouwer et al., 2015; Cheng et al., 2021). Physical parameters of ripples (morphology, length, and amplitude) also provide useful information for facies analysis, delineation of paleo-shore line, and evaluating hydrological characteristics of the basin and sediment transport (Harms, 1969; Tanner, 1970; Komar, 1976; Allen, 1984; Baas, 1999). The studies on ripple marks are based mainly on the recent siliciclastic deposits, using also experimental data and empirical morphological parameters. Ancient ripple marks are often poorly preserved due to post-sedimentation erosion (Romanovski, 1977; Allen, 1984). Although the application of ripples in deducing the sedimentary environment has been questioned because similar ripples could form at highly variable depths (Kindle and Bucher, 1926; Romanovski, 1977; Allen, 1984), and ripple size may not correctly elucidate the depth of water (Ewans, 1942), ripples are one of the most popular tools in working out sedimentation conditions. Despite their suitability for working out the sedimentary process, the poor preservation potential of ripples is a deterrent. They tend to get eroded and obliterated during the post-depositional processes and, therefore, are not abundant in nature. These structures are usually destroyed during the metamorphic reconstitution; therefore, quartzite is usually an unlikely candidate for such studies. However, wave-formed ripples in Proterozoic quartz arenites have been successfully used for Paleoenvironmental reconstruction in several studies (Clifton and Dingler, 1984; Aspleri, et al., 1994) including numerical estimates of water depth of ancient waves (Tanner, 1971). Cross bedding structures are used as a tool to decipher plaeo-tectonics and sedimentation history of Proterozoic Alwar Group. Such types of planer structures studies were also conducted for Gulcheru quartzite of Cuddapah basin (Sukanta et al., 2017).

The Mesoproterozoic quartzites exposed in a road section in the Jamwa Ramgarh area of Rajasthan in NW India display a variety of well-preserved ripple marks at several planes despite the rocks having undergone low to medium-grade metamorphism and recrystallization (Fig. 1). The

quartzite belongs to the Alwar Group of the Delhi Supergroup. The development of a large variety of ripple marks and diversity in their morphological parameters (shape, size, and amplitude). Therefore, it can be regarded as a unique site where maximum possible ripple types are exposed within sediment sequence of less than 2 m, implying rapidly changing depositional conditions due to unusual fluctuations in wave amplitude, energy and direction. This paper presents a detailed inventory of the Jamwa Ramgarh ripple marks and documents their megascopic characteristics. Morphological parameters of all ripple types were analysed for quantitative estimation of paleodepth and paleo-wave period along with orbital diameter and maximum wave period. The findings have been discussed to decipher the depositional environment at the southern margin of the Alwar – Jaipur sub-basin.

REGIONAL GEOLOGY AND STRATIGRAPHY

The NW Indian block, also known as the Aravalli Craton, is constituted by an Archean basement, the Banded Gneissic Complex (BGC - Heron, 1953) dated to 3.3 to 2.5 Ga (Roy and Kroner, 1996; Widenecke et al., 1996), over which supracrustal sequences of Aravalli (Paleoproterozoic) and Delhi (Meso-Neoproterozoic) Supergroup rocks were deposited (Roy and Jakhar, 2002; Deb and Thorpe, 2004; McKenzie et al., 2013). A Paleo- Mesoproterozoic Vindhyan Supergroup (Rasmussen et al., 2002; Ray et al., 2002; Gregory et al., 2006) occurs to the east of the Aravalli – BGC juxtaposed along a major fault, named the Great Boundary Fault (Fig. 1).

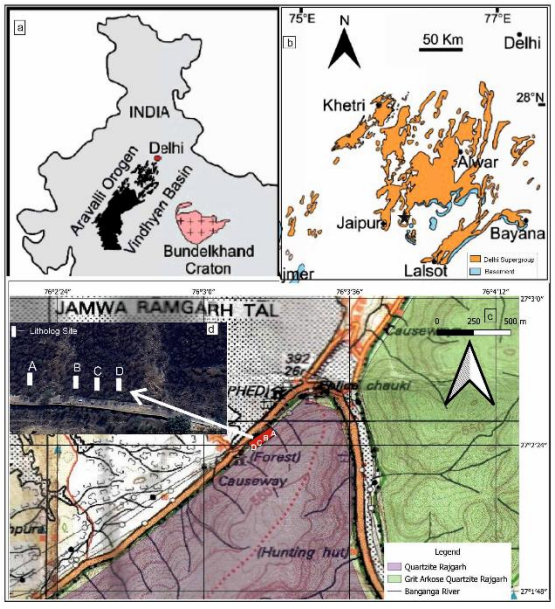

Figure 1 **a.** Location map of Aravalli Craton, NW India **b.** Geological map of North Delhi Fold Belt (Roy, 1988), **c.** Geological map of Jamwa Ramgarh section with study area, **d.** Google Earth image of study area

Delhi Supergroup, the dominant lithostratigraphic unit of the Aravalli Craton, was subdivided by Sinha Roy (1984) into two geographic domains, i.e. North Delhi Fold Belt (NDFB - older) and South Delhi Fold Belt (SDFB - younger). The diachronous sedimentation history, based entirely on the age of intrusive granites, was contested by some later workers (Bose et al., 1996; Roy and Kataria, 1999), however, more recent detrital zircon geochronologic studies support a diachronous sedimentation for the Delhi Supergroup (Wang et al., 2017). The NDFB is further subdivided into three, fault-bound, sub-parallel basins, namely, the Bayana-Lalsot, Alwar-Jaipur, and Khetri sub-basins (Sinha-Roy et al., 1998), from east to west. The Raialo Group (dolomitic limestone, quartzite and mafic volcanics) represents the oldest stratigraphic unit of the NDFB, followed by Alwar Group (arenaceous) and Ajabgarh Group (argillaceous – arenaceous facies), in stratigraphically ascending order (Gupta et al., 1997). Jamwa – Ramgarh, the area of present study, forms the southern part of the Alwar-Jaipur sub-basin (Fig. 1). Stratigraphy of the area is listed in Table 1.

Table-1a Stratigraphy of Delhi Supergroup

Supergroup	Group	Formation	Thickness (after Singh 1982)
Delhi Su-pergroup	Ajabh-garh	Bharkhol	100- 150m+
		Thanagazi	100 – 150m+
		Sariska	90- 150m+
		Kushalgarh	110- 200m+
	Alwar	Pratapgarh	900m+
		Kankanwari	100-250m
		Rajgarh	40- 1200m+
	Raialo	Tehla	1500 – 2020m+
		Serrate	200- 300m+

Table- 1b Lithology of Rajgarh Formation

Formation	Lithology
Rajgarh	Quartz-biotite schist with conglomerate **Quartzite** Dolomite Quartzite with basic flows at places Grit, Arkose, Quartzite Conglomerate with pebbly quartzite

STRATIGRAPHY OF JAMWA RAMGARH AREA

Stratigraphically, the Alwar- Jaipur sub-basin consists of Serrate and Tehla formations of the Raialo Group, Rajgrah, Kankwarhi and Pratapgarh formations of Alwar Group and Kushalgarh, Sariska, Thanagazi, and Bharkol formations of Ajabhgarh Group.

The studied quartzites (quartz arenite) belongs to the Rajgarh Formation of Alwar Group (Table 1). These quartz arenites are exposed along a

Table- 2 Morphological parameters of studied ripple marks in Jamwa Ramgarh quartz arenite									
Sr. No.	**Amplitude (H)**	**Wave Length (S)**	**RS = H/S**	**RI = S/H**	**Angle**	**d_0**	**Tm (Sec)**	**Wave height (cm)**	**Water Depth (cm)**
Small									
1	0.3	3	0.10	10	35	4.62	1.11	2.54	21.85
2	0.3	4	0.08	13.33	40	6.15	1.35	4.43	25.04
3	0.4	2.5	0.16	6.25	51	3.85	0.99	1.60	20.41
4	0.4	4	0.10	10	358	6.15	1.35	4.43	25.04
5	0.5	1.4	0.36	2.8	348	2.15	0.70	0.38	18.50
6	0.5	1.4	0.36	2.8	75	2.15	0.70	0.38	18.50
7	0.5	2.5	0.20	5	18	3.85	0.99	1.60	20.41
8	0.5	3.5	0.14	7	16	5.38	1.24	3.49	23.39
9	0.5	3.5	0.14	7	16	5.38	1.24	3.49	23.39
10	0.5	4	0.13	8	56	6.15	1.35	4.43	25.04
11	0.25	1.5	0.17	6	19	2.31	0.73	0.57	18.75
12	0.5	2.4	0.13	8	28	3.69	0.96	1.41	20.13
13	0.5	4	0.13	8	38	6.15	1.35	4.43	25.04
14	0.5	4	0.13	8	18	6.15	1.35	4.43	25.04
15	0.5	4	0.13	8	38	6.15	1.35	4.43	25.04
16	0.5	4.5	0.11	9	334	6.92	1.46	5.38	26.81
17	0.5	4.5	0.11	9	334	6.92	1.46	5.38	26.81
18	0.5	5	0.10	10	55	7.69	1.57	6.32	28.70
19	0.5	5	0.10	10	92	7.69	1.57	6.32	28.70
20	0.5	5	0.10	10	60	7.69	1.57	6.32	28.70
21	0.5	7	0.07	14	2	10.77	1.96	10.10	37.70
22	0.5	9	0.06	18	127	13.85	2.32	13.88	49.52
Medium									
1	0.6	4	0.15	6.67	74	6.15	1.35	4.43	25.04
2	0.6	4	0.15	6.67	55	6.15	1.35	4.43	25.04
3	0.6	4.5	0.13	7.50	340	6.92	1.46	5.38	26.81
4	0.7	3	0.23	4.29	20	4.62	1.11	2.54	21.85
5	0.8	3.5	0.23	4.38	32	5.38	1.24	3.49	23.39
6	0.8	4.5	0.18	5.63	6	6.92	1.46	5.38	26.81

7	0.9	3	0.30	3.33	40	4.62	1.11	2.54	21.85
8	1	4	0.25	4.00	12	6.15	1.35	4.43	25.04
9	1	4	0.25	4.00	17	6.15	1.35	4.43	25.04
10	1.1	6	0.18	5.45	30	9.23	1.77	8.21	32.89
11	1.1	4.7	0.23	4.27	20	7.23	1.50	5.75	27.55
Large									
1	0.6	2.5	0.24	4.17	38	3.85	0.99	1.60	20.41
2	0.6	5.5	0.11	9.17	50	8.46	1.67	7.27	30.72
3	0.7	7	0.10	10.00	11	10.77	1.96	10.10	37.70
4	0.8	6	0.13	7.50	350	9.23	1.77	8.21	32.89
5	0.8	6.8	0.12	8.50	81	10.46	1.92	9.72	36.69
6	1	5.5	0.18	5.50	26	8.46	1.67	7.27	30.72
7	1	5.5	0.18	5.50	31	8.46	1.67	7.27	30.72
8	1	6	0.17	6.00	26	9.23	1.77	8.21	32.89
9	1	6.5	0.15	6.50	45	10.00	1.87	9.16	35.21
10	1	7	0.14	7.00	345	10.77	1.96	10.10	37.70
11	1	7.5	0.13	7.50	25	11.54	2.05	11.05	40.36
12	1	8	0.13	8.00	28	12.31	2.14	11.99	43.21
13	1.1	6	0.18	5.45	30	9.23	1.77	8.21	32.89
14	1.1	7.5	0.15	6.82	16	11.54	2.05	11.05	40.36
15	1.2	6	0.20	5.00	14	9.23	1.77	8.21	32.89
16	1.2	7	0.17	5.83	69	10.77	1.96	10.10	37.70
17	1.2	12	0.10	10.00	105	18.46	2.81	19.55	74.56
18	1.4	6	0.23	4.29	9	9.23	1.77	8.21	32.89
19	1.4	8	0.18	5.71	65	12.31	2.14	11.99	43.21
20	1.4	11.5	0.12	8.21	27	17.69	2.73	18.61	69.65
21	1.4	21	0.07	15.00	31	32.31	4.08	36.56	254.49
22	1.5	6	0.25	4.00	28	9.23	1.77	8.21	32.89
23	1.5	8	0.19	5.33	25	12.31	2.14	11.99	43.21
24	1.5	9	0.17	6.00	355	13.85	2.32	13.88	49.52
25	1.5	10.5	0.14	7.00	21	16.15	2.57	16.72	60.77
26	1.7	17.5	0.13	8.00	51	26.92	3.61	29.95	157.88

27	1.5	19	0.08	12.67	109	29.23	3.82	32.78	193.73
28	1.6	7	0.23	4.38	18	10.77	1.96	10.10	37.70
29	1.6	7.5	0.21	4.69	18	11.54	2.05	11.05	40.36
30	1.7	7	0.24	4.12	23	10.77	1.96	10.10	37.70
31	1.8	9.5	0.19	5.28	23	14.62	2.40	14.83	53.02
32	1.8	10	0.18	5.56	23	15.38	2.49	15.77	56.76
33	1.9	13	0.15	6.84	42	20.00	2.96	21.44	85.46
34	2	8	0.25	4.00	10	12.31	2.14	11.99	43.21
35	2	8.5	0.24	4.25	6	13.08	2.23	12.94	46.26
36	2	10	0.20	5.00	44	15.38	2.49	15.77	56.76
37	2	11	0.18	5.50	27	16.92	2.65	17.66	65.06
38	2	13	0.15	6.50	44	20.00	2.96	21.44	85.46
39	2.2	14	0.16	6.36	40	21.54	3.11	23.33	97.95
40	2.3	15	0.15	6.52	330	23.08	3.26	25.22	112.26
41	2.5	8.5	0.29	3.40		13.08	2.23	12.94	46.26
42	2.5	11	0.23	4.40	16	16.92	2.65	17.66	65.06
43	2.5	12	0.21	4.80	27	18.46	2.81	19.55	74.56
44	2.6	12.5	0.21	4.81	18	19.23	2.89	20.50	79.83
45	2.8	16	0.18	5.71	8	24.62	3.40	27.11	128.67
46	2.8	18	0.16	6.43	20	27.69	3.68	30.89	169.03
47	3	11.5	0.26	3.83	30	17.69	2.73	18.61	69.65
48	3	13	0.23	4.33		20.00	2.96	21.44	85.46
49	3.1	19	0.16	6.13	58	29.23	3.82	32.78	193.73
50	3.2	10	0.32	3.13	16	15.38	2.49	15.77	56.76
51	3.3	20	0.17	6.06	37	30.77	3.95	34.67	222.04
52	3.6	20	0.18	5.56	15	30.77	3.95	34.67	222.04
53	3.7	25	0.15	6.76	92	38.46	4.58	44.12	439.16
54	3.8	18	0.21	4.74	21	27.69	3.68	30.89	169.03
55	4.5	24	0.19	5.33	44	36.92	**4.46**	42.23	383.16
Mega									
1	4.0	27	0.15	6.75	19	41.54	4.82	47.90	576.90
2	4.0	60	0.07	15.00	118	92.31	8.21	110.27	51992.85

3	4.2	27	0.16	6.43	22	41.54	4.82	47.90	576.90
4	4.5	35	0.13	7.78	16	53.85	5.73	63.02	1717.91
5	5.1	50	0.10	9.80	55	76.92	7.27	91.37	13291.25
6	5.3	35	0.15	6.60	35	53.85	**5.73**	63.02	1717.91

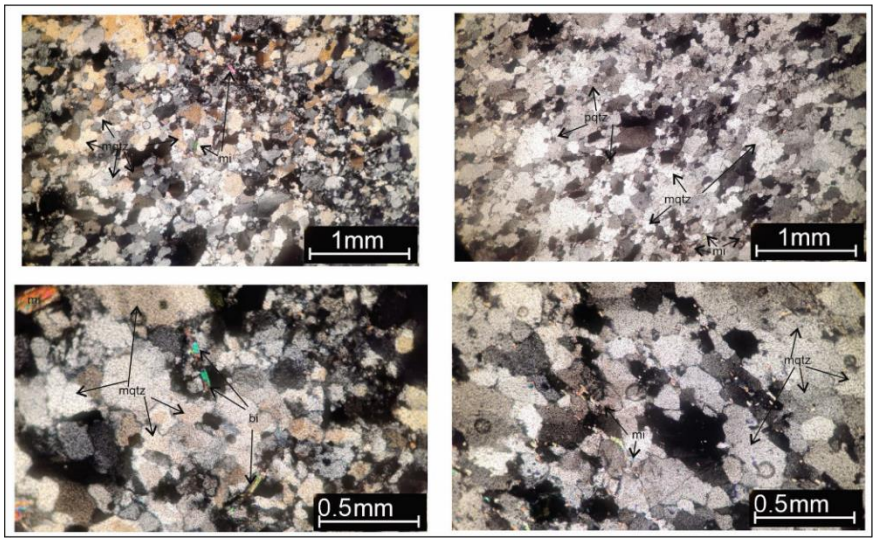

Figure 2 Photomicrograph of Rajgarh quartzite of Jamwa Ramgarh section, mqtz- monocrystalline quartz, pqtz- polycrystalline quartz, mi- muscovite

road section at the Jamwa Ramgarh reservoir, situated eastern side of Jaipur city (Fig. 1). The Rajgrah Formation, in Alwar- Jaipur basin, is marked by conglomerates and pebbly quartzites at the base, grading into coarse to medium grain (gritty to arkosic quartzite- DR map) and quartzite with basic flows at places, dolomite, massive quartzites and the uppermost litho-unit is a quartz-biotite schis with conglomerate (Gupta et al., 1997). The main direction of sediment transport was towards north-northwest for Rajgarh Formation. The massive quartzites at Jamwa Ramgarh host well-preserved ripple marks at several, still-preserved bedding planes.

FIELD AND LABORATORY METHODS

The study includes geological investigations along 250m travers near Jamwa Ramgarh reservoir which shows the best development of diverse types of ripple structures in quartz arenite. Detailed field studies comprising documentation of sedimentary features, orientation of planer structures and description of morphometric parameters of ripple mark at four spots A, B, C and D (Fig. 1). A total of ninety-four ripple marks (ripple surfaces) were documented from massive quartzite in Jamwa Ramgarh section. All ripples are preserved in a single direction along the road side. The strike is E 50- 55° N with moderate dips (20° to 40°) towards NW. They were studied in detail over a strike length of 250 m, where they show prolific development. The data of all ninety-four ripple marks is collected manually with the help of measuring tape and scale. Petrographic characters were observed and examined under a polarizing microscope. Based on field variation in term of variation in colour and texture, total fifteen samples were selected to examine grain size, texture and mineralogical features.

RESULTS

The thickness of individual quartzite bed varies from 2 to 50 cm. The petrographic studies of quartzite reveal uniformity in grain size, sorting,

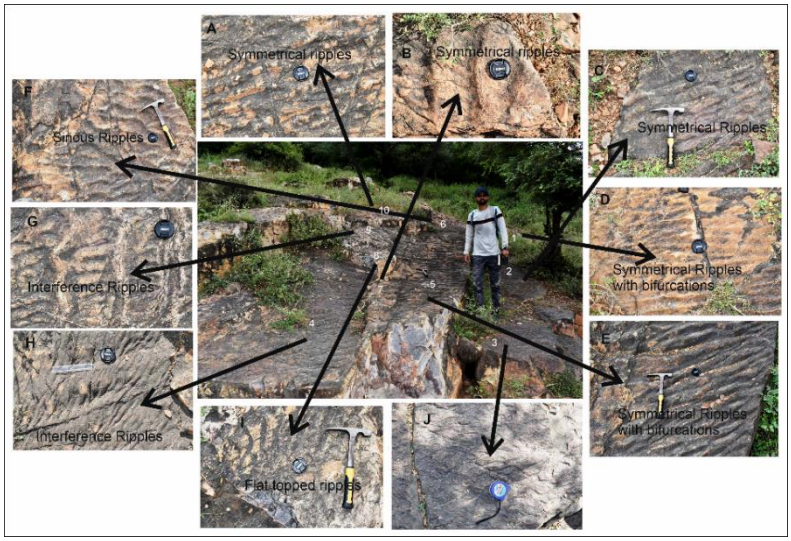

Figure 3 Field Photographs showing variety of ripple marks at site A (refer to Fig. 1): A, B & C – symmetrical ripples, D & E- symmetrical ripples with bifurcations, F- sinuous ripples, G & H- Interference ripples, I- flat-topped ripples

roundness and composition (Fig. 2). In general, grain size varies from 0.25 mm to 0.45 mm with an average 0.35 mm. The quartz grains, the most dominant minerals, are well sorted and sub-rounded, in addition <5 % phyllosilicates are also present. The monocrystalline quartz is dominant in comparison to polycrystalline quartz (Fig. 2).

RIPPLE MORPHOLOGY

The ripple morphometric data are provided in Table 2, wherein Wave length (S) is the horizontal distance from crest to crest between adjacent ripples, H is the vertical length (amplitude) from crest to trough. Vertical Form Index (VFI) or Ripple Index (RI) represents the ratio between wave length and amplitude (S/H), and Ripple Steepness (R.S.) is derived by the ratio of amplitude and wavelength (H/S). Orbital diameter (d_0) is the maximum distance of water particles move as wave passes. The orbital diameter is calculated by: d_0= S/ 0.65 (Miller and Komar, 1980) for symmetric orbital ripples near sediment- water interface. Tm is the maximum wave period that can yield bottom velocities above the threshold for initiation of movement for grain size

Figure 4 Field Photographs showing variety of ripple marks at site B (refer to Fig. 1): A– symmetrical ripples, B & C- symmetrical ripples with bifurcations, D-sinuous ripples and E- pointed crest and rounded trough ripples.

(D). It is calculated by 0.17 × (d_0^2/D)1/3 (in cm and seconds) (Dingler, 1979). The average values of these parameters are provided in the Table 2.

RIPPLE CLASSIFICATION

Ripples are classified on the basis of a combination of morphological parameters, such as the Ripple Wave length (S) and Amplitude (H). The ripples with amplitude <0.5 cm, considered as 'small ripples'. Ripples wavelength from 2.5 to 5 cm considered as 'medium ripples' and wave length > 5.0 cm considered as 'large ripples' (Aspleri et al., 1994). Ripples with wave length >25cm are named 'Very Large Ripples' or Mega Ripples. As per this criterion, out of total studied ripples, 59% of are classified as large, 24% as small, 12% as medium, and remaining 5% as very large ripples (Table 2).

The ripples are predominantly symmetric (straight crest) type (Fig. 3a, b and c; Figs. 4a, 5a and

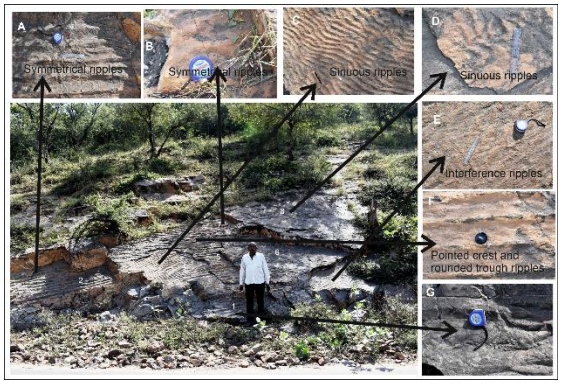

Figure 5 Field Photograph showing variety of ripple marks at site C (refer to Fig. 1): A & B – symmetrical ripples, C & D- sinuous ripples, E- Interference ripples, F- pointed crest and rounded trough ripples

Figure 6 Field Photograph showing variety of ripple marks at site D (refer to Fig. 1): A, B & C - symmetrical ripples, D- symmetrical ripples with bifurcations, E- Pointed crest and trough ripples, F- flat-topped ripples, G- pointed crest and rounded trough ripples

Figure 7 Field Photographs showing other types of ripple marks in the study area: A – Pointed crest and trough ripples, B- flat-topped ripples, C- catenary ripples, D & E- mega ripples, F- current ripples, G- criss-cross ripples, H- road side view of exposure

b; and 6 a, b, and c) and show further variations, such as bifurcation types (Figs. 3d and e, 4b and c, and 6d), sinuous (curved crest) ripples (Figs. 3f, 4d, 5c

and d), interference ripples (Figs. 3g and h and 5e), pointed crest and pointed trough ripples (Figs. 6e and 7a,), flat topped ripples (Figs 3i, 6f, and 7b), pointed crest with rounded trough ripples (Figs. 4e, 5f, and 6g), catenary ripples (Fig. 7c) and mega ripples (Fig. 7d and e). Apart from these types, asymmetric current ripples (Fig. 7f) and criss-cross ripples (Fig. 7g) are also present.

RIPPLE SHAPE

The shape of ripples can be explained with the help of ripple symmetry, ripple index and ripple steepness. The ripple index (RI) values (Table 2) range from 2.8 to 15.0 with an average 6.8, significantly below the values for wind ripples (VFI > 15; Tanner, 1967). The majority of ripples are symmetric, indicating either current or wave dominated environment. The ripples are straight, long-crested, two-dimensional forms and interference ripples are also common. The average ripple steepness values for small, medium, large and very large ripples are 0.14, 0.21, 0.18 and 0.13, respectively. Occasional criss-cross ripples, catenary ripples, current ripples and flat-topped ripples were also observed.

RIPPLE CREST LINE

The ripple crust line is an indicator of the paleocurrent direction as it is oriented parallel to the wave front. The orientation crest line of all studied ripple marks are ranges between 330° and 109° but maximum number of ripples are aligned between 6° and 45°N. Majority of small ripples range between 16° and 19°N and medium ripples between 6° and 20°N. Large ripple crest line is aligned mainly between 21° and 37°N (Fig. 8).

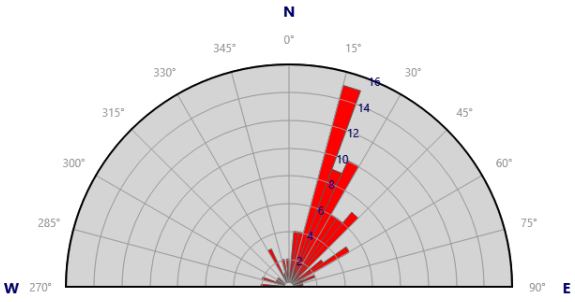

Figure 8 Rose diagram showing orientation of Ripples crest lines underling maximum ripples aligned in NE- SW direction.

VERTICAL DISTRIBUTION OF BEDS AND VARIATION IN RIPPLE MARKS

The vertical description of quartzite beds with ripple marks at four sites namely A, B, C and D (Fig. 9) is described as below:

Site A: This site comprises a total thickness of 112 cm with ten ripples including three small ripples, two interference ripples and five large ripples. The small ripples are aligned in 334° to 34° and large ripples in 26° to 69° direction. Their amplitude and wave length varies from 0.4 to 0.5 cm and 4 to 4.5 cm, respectively for small ripples and from 1.1 to 3.1cm and 6 cm to 19 cm, respectively for large ripples. The exposed thickness of lowest bed with small ripples is 35 cm, and it is overlain by large ripples (symmetrical) of 2 cm thickness. These are

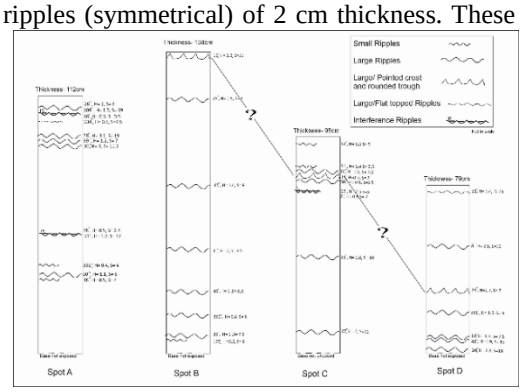

Figure 9 Vertical bed description for sites A, B, C & D, showing ripples types exposed on different beds.

further overlain by small ripples (symmetrical) with 5 cm thickness. The next bed is 15 cm thick and marked by interference ripples. These ripples are overlain by large (symmetrical) ripples contained within a 40 cm thick bed, followed upward by a 2 cm thick bed having large, sinuous ripples (sinuous). It is overlain by large ripples (symmetrical). Seven cm thickness was measured for next bed which contains flat-topped, small ripples. It is overlain by a second set of interference ripples contained in a 2 cm thick bed. The uppermost, 2 cm this bed, displays large ripples.

Site B: The complete column thickness of 138 cm contains eight ripples comprising one small ripple and seven large ripples. The large ripples are aligned in 350°N to 65° N direction, their amplitude ranges between 0.8 and 2.5 cm and wave length varies from 6 to 11 cm. The exposed thickness of lowermost small ripple (sinuous) is 7cm. It is overlain by 3 cm thick, large ripples (symmetrical with bifurcation). The subsequent bed with similar large ripples, is 8 cm thick, followed by a 10 cm thick one. Further up section, large ripples (symmetrical) are exposed on beds of 20 cm, 30 cm, and 40 cm thickness. The uppermost bed is 40 cm thick and contains large ripples (pointed crest with rounded trough).

Site C: This comprises a total thickness of 95 cm with nine ripples comprising three small and six large ripples. The small ripples are aligned in 2°N to 92°N direction, with amplitude between 0.4 and 0.5 cm, and wave length between 2.5 to 7 cm. The large ripples are aligned in 11°N to 50°N directions, with significant variable amplitude fluctuating between 0.6 and 1.8 cm, and wave length from 5.5 to 11 cm. The exposed thickness of lowest bed is 10 cm having large ripples. It is overlain by a 35 cm thick bed with large ripples (symmetrical). Further upward, the 30

cm thick bed has large are sinuous types with a thickness of 5 cm. It is overlain by a 1.5 cm thick bed with large ripples (pointed crest and rounded trough). It is overlain by large ripples of a 2 cm thick bed. The next bed with small ripples is also 1.5 cm thick with small ripples (symmetrical) and the uppermost small ripple (sinuous) bed has 10 cm thickness.

Site D: This section comprises seven large ripples in a 80 cm column thickness. These ripples are aligned in 355°N to 42° N direction and their amplitudes range between 1.5 and 2.8 cm, and wave length from 7 to 18 cm. The lowermost ripple (symmetrical) is contained in a 1 cm thick bed, which is overlain by a 8 cm thick bed with symmetrical ripples. The thickness of next bed is 2 cm, which in turn, is overlain by a 13 cm thick bed with large ripples (pointed crest and trough). it is overlain by a 10 cm thick bed with pointed crest and rounded trough ripples. The next 20 cm thick bed contains symmetrical ripples while the uppermost, 25 cm thick bed exposes flat topped large ripples.
A correlation among these sites is unclear, however, the pointed crest and rounded trough ripples are common at site B, C and D. These show a lateral continuity; however, a direct correlation seems unlikely due to lack of supporting evidence.

DISCUSSION

PALEODEPTH AND PALEO-WAVE CONDITIONS

Relevant morphological parameters, Wave height (H) and Water depth (h) were calculated by using the formula of Tanner (1971) below:

$$H = 38.52 + 1.89 \times S - 7.11 \times \ln D$$
$$\ln h = 14.64 + 0.61 \times S - 2.45 \times \ln D - 0.28 \times \lambda$$

Wherein, S is the ripple wave length, D is grain size, λ is water wavelength. The minimum water depth for wave propagation is 4.3 cm (Tricker, 1965). The water wavelength (λ) was estimated by the formula: $\Lambda = 33.77 + 1.72\ S - 7.22\ \text{In h}$ (Tanner 1971). Since sedimentary structures (ripple marks) are well preserved, we assume that the rock did not undergo significant recrystallization. Therefore, the grain size of quartz can be considered to represent original grain size. The quartz grain shows a correspondence with the size of ripples and progressively increased from small, medium to large - very large ripples. Very large ripples are comprised by largest grains. The estimated wave height for small ripples ranges from 1.59 cm (minimum) to 13.88 cm (maximum) with an average of 4.37 cm. Similarly, the medium ripples show an overlap and range between 2.54 and 8.21 cm with an average of 4.64 cm. In the case of large ripples, the wave height ranges from 1.60 to 44.12 cm with an average of 13.33 cm, while in case of very large ripples it ranges from 47.90 to 110.27 cm with an average of 70.58 cm.

Bartholdy et al. (2015) suggested that the logarithmic velocity profile, grain-size and flow depth have a direct impact on the formation of ripples. In the present study, water depth calculations shows, a range between 17.56 and 49.52 cm with an average value of 25.66 cm for small ripples, between 21.85 and 32.89 cm with an average of 25.57cm for medium ripples, from 20.41 to 439.16 cm with an average of 85.55 cm for large ripples and 576.90 cm to 51.99 m with an average of 11.6 m for very large ripples. The average wave height and water depth for all three types of ripples are 24.23 cm and 2.9 m respectively (Table 3).

Table-3 Average values of statistical parameters of ripples in Jamwa Ramgarh quartz arenite

Parameters	small (n=22)	Medium (n=11)	Large (n=55)	Very Large (n=6)	Total (n =94)
H	0.46	0.84	1.87	4.52	1.92
S	3.90	4.11	10.92	39.00	14.48
RI	8.64	5.11	6.16	8.73	7.16
RS	0.14	0.21	0.18	0.13	0.16
d_0	5.99	6.32	16.81	60.00	22.28
Tm	2.81	2.95	5.55	13.14	6.11

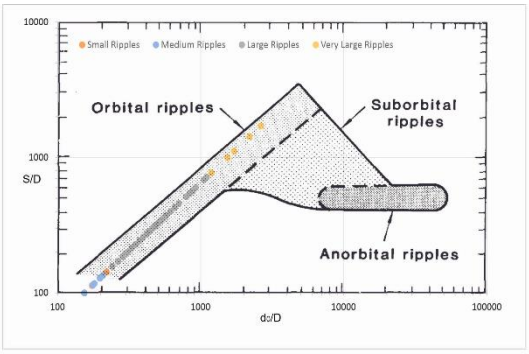

Figure 10 Plot of ratio of ripple wave length to grain size against ratio of orbital diameter to grain size (Clifton and Dingler, 1984) showing orbital ripple affinity for all ripples in the study area.

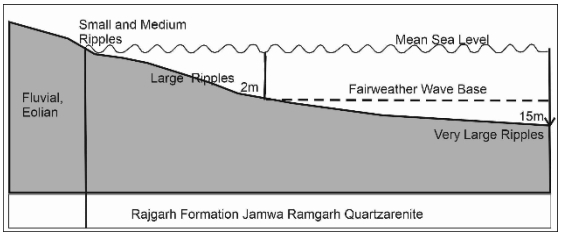

Figure 11 Plot depicting low energy coastal profile for the studied ripples.

On the basis of relationship between ripple wave length and orbital diameter, Clifton (1976) subdivided symmetrical ripples into three types i.e., orbital ripples, suborbital ripples and an-orbital ripples, The Jamwa Ramgarh ripple data were plotted to discriminate them (Fig. 10) and all the sample plot in the orbital ripple field. Their d_0/D ratios for small ripples ranges between 72 and 396 with an average of 173, from 132 to 264 with an average of 181 for medium ripples, from 110 to 1099 with an average of 480 for large ripples, and

from 1187 to 2637 with an average of 1714 for very large ripples. Due to the requirement of short oscillatory motion, the orbital ripples most commonly occur in very shallow water conditions, under short period waves (Pedocchi and García, 2009; Bartholdy et al., 2015). Pedocchi and García (2009) suggested that the sediment size has an important effect on the size and geometry of bed forms that can be generated by oscillatory flows. Alternatively, Aldridge et. al. (2015) recommended that the distribution of highest-level disturbance, where mega ripples formed, showed a complex relationship between water depth, tidal stress, wave fetch and grain size.

Table-4 Calculated wave parameters and water depth of Jamwa Ramgarh quartz arenite

Ripples	Wave Length (cm)	Wave Height H (cm)	Water Depth h (cm)
Small	3.90	4.38	25.60
Medium	4.11	4.64	25.57
Large	10.92	17.52	87.06
Very Large	39.00	70.58	11645.62
Average	14.48	24.28	2945.96

The wave ripple crest are reliable indicators of paleo-shoreline trend as the incoming waves of variable trend become realigned parallel to the shoreline. The position of symmetrical wave ripples with an average wave height of 24.2 cm and average water depth of 2.9 m can be classified as beach sand at shallow marine area. The large long period waves cannot be supported by such water depth. The wave period for small ripples ranges from 1.52 to 4.99 seconds with an average of 2.81 seconds, from 2.40 to 3.81 seconds with an average of 2.95 seconds for medium ripples, from 3.60 to 9.87 with an average 5.61 seconds for large ripples, and from 10.39 to 17.69 with an average of 13.14 seconds for very large ripples. The average wave period for all these ripples is 6.13 seconds. The large and very large ripples are formed in slightly deeper continental shelf area (Fig. 11). Allen (1984) described a close relationship of ripple morphology, water depth and wave velocity. In the Jamwa Ramgarh area, very large ripples can be associated with higher water depth, courser grain size, higher wave height and long wave periods.

The presence of criss-cross and interference ripples shows waves from different weather systems meet each other almost at the right angle. They indicate two dominant paleocurrent directions. Sinusoidal profile of many ripples indicates an environment with weak currents where water motion is dominated by wave oscillations (Boggs, 2006).

CONCLUSION:

1) On the basis of ripple wave length and amplitude, four types of ripples are observed in the study area i. e. small, medium, large and mega ripples.
2) The main direction of sediment transport was from north-northwest during the formation of ripples.
3) The total thickness of the quartzite containing ripples marks is consistently small and indicates an average water depth of less than 3 m.
4) The wave periods in case of small, medium and large ripples are generally short (approx. 6 seconds) to ensure bottom orbital velocities adequate for sediment movement.
5) The maximum distance water particle can move as wave passes, is approximately 17 cm.
6) The wave period for very large ripples is approx. 13 seconds and the maximum distance the water particle can move as wave passes is approx. 60 cm.
7) Continental shelf with variable depth is proposed for development of these wave ripples.

REFERENCES

Allen, J.R.L. (1984). Sedimentary Structures, Their Character and Physical Basis: vol. 1. Elsevier Scientific Publ. Co., Amsterdam, 593p.

Aldridge, J.N., Parker, E.R., Bricheno, L.M., Green, S.L. and Van der Molen, J. (2015). Assessment of the physical disturbance of the northern European Continental shelf seabed by waves and currents. Continental Shelf Research, vol. 108, pp. 121-140.

Aspler, L.B., Chiarenzelli, J.R. and Bursey, T.L. (1994). Ripple marks in quartz arenites of the Hurwitz Group, Northwest Territories, Canada; evidence for sedimentation in a vast, early Proterozoic, shallow, fresh-water lake. Journal of Sedimentary Research, vol. 64 (2a), pp. 282-298.

Baas, J.H. (1999). An empirical model for the development and equilibrium morphology of current ripples in fine sand. Sedimentology, vol. 46, pp. 123-138.

Baird, D.M. (1962). Ripple marks. Journal of Sedimentary Research, vol. 32(2), pp. 332-334.

Bartholdy, J., Ernstsen, V. B., Flemming, B. W., Winter, C., Bartholomä, A., and Kroon, A. (2015). On the formation of current ripples. Scientific Reports, vol. *5* (1), pp. 11390.

Bergman, C. (1979). Ripple marks in the Silurian Gotland Sweden. Geologiska Foreningen Stockholm Forrhandlingar.

Boggs, S. (2006). Principles of sedimentology and stratigraphy (Vol. 662). Upper Saddle River, NJ: Pearson Prentice Hall.

Bose, U., Mathur, A.K., Sahoo, K.C., Bhattacharya, S., Dutt Krishan Kumar, A.V., Sarkar, S. S., Choudhary, S. and Choudhary, I. (1996). Event stratigraphy and physicochemical characters of B.G.C and associated supracrustals in the south Mewar plains of Rajasthan. Journal of the Geological Society India, vol. 47, pp. 325-338.

Chang, T.S. and Flemming, B.W. (2013). Ripples in intertidal mud—a conceptual explanation. Geo-Marine Letters, vol. 33, pp. 449-461.

Cheng, C.H., De Smit, J.C., Fivash, G.S., Hulscher, S.J., Borsje, B.W. and Soetaert, K. (2021). Sediment shell-content diminishes current-driven sand ripple development and migration. Earth Surface Dynamics Discussions, vol. 9 (5), pp. 1335-1346.

Clifton, H.E. (1976). Wave-formed sedimentary structures—a conceptual model; In: R.A. Davis, R.L. Ethington (Editors), Beach and Nearshore Processes. Society of Economic Paleontology and Mineralogy, Special Publications, vol. 24, pp. 126-148.

Clifton, H.E. and Dingler J.R. (1984). Wave-formed structures and Paleoenvironmental Reconstruction. Marine Geology, v. 60, pp. 165-198.

DR map (2022). District Resource Map of Jaipur District, Geological Survey of India.

De Vleeschouwer, D., Leather, D. and Claeys, P. (2015). Ripple marks indicate mid-Deonian paleo-wind directions in the Orcadian Basin (Orkney Isles Scotland). Palaeogeography, Palaeoclimatology, Palaeoecology, vol. 426, pp. 68-74.

Deb, M. and Thorpe, R.I. (2004). Geochronological constraints in the Precambrian Geology of Rajasthan and their Metallogenic implications In: Deb M. Goodfellow WD (Eds) Sediment-hosted Lead–Zinc Sulphide Deposits. Narosa Publishing House New Delhi, pp. 246-263.

Dingler, J.R. (1979). The threshold of grain motion under oscillatory flow in a laboratory wave channel. Journal of Sedimentary Research, vol. 49(1), pp. 287-293.

Ewans, O.F. (1942). The relation between the size of wave formed ripple marks, depth of water, and the size of the generating waves. Journal of Sedimentary Petrology, vol. 12, pp. 31-35.

Gregory, L.C., Meert, J.G., Pradhan, V., Pandit, M.K., Tamrat, E. and Malone, S. J. (2006). A paleomagnetic and geochronologic study of the Majhgawan Kimberlite India: implications for the age of the Upper Vindhyan Supergroup. Precambrian Research, v. 149, pp. 65-75.

Gupta, P., Arora, Y.K., Mathur, R.K., Iqbaluddin, Prashad, B., Sahai, T.N. and Sharma, S.B. (1997). Lithostratigraphic map of the Aravalli region southern Rajasthan and northeastern Gujarat. Geological Survey of India Publications, Jaipur, vol. 123, pp. 262.

Harms, J.C. (1969). Hydraulic significance of some sand ripples. Geological Society of America Bulletin, vol. 80 (3), pp. 363-396.

Heron, A.M. (1953). Geology of central Rajasthan. Mem. Geol. Surv. India, v.79, 389p.

Kindle, E.M. and Bucher, W.H. (1926). Ripple mark and its interpretation. Treatise on Sedimentation, pp. 451-483.

Komar, P.D. (1976). Beach Processes and Sedimentation. Prentice-Hall Inc Englewood Cliffs New-Jersey 429p.

McKenzie, N.R., Hughes, N.C., Myrowc, P.M., Banerjee, D.M., Deb, M. and Planavskye, N. J. (2013). New age constraints for the Proterozoic Aravalli–Delhi successions of India and their implications. Precambrian Research, vol. 238, pp. 120-128.

Miller, M.C. and Komar, P.D. (1980). Oscillation sand ripples generated by laboratory apparatus. Journal of Sedimentary petrology, vol. 50, pp. 173-182.

Pedocchi, F. and García, M.H. (2009). Ripple morphology under oscillatory flow: 1. Prediction. Journal of Geophysical Research, Oceans, 114(C12).

Rasmussen, B., Bose, P.K., Sarkar, S., Banerjee, S., Fletcher, I.R. and McNaughton, N.J. (2002). 1.6 Ga U-Pb zircon age for the Chorhat Sandstone lower Vindhyan India: Possible implications for early evolution of animals. Geology, vol. 30, pp. 103-106.

Ray, J., Martin, M.W., Veizer, J. and Bowring, S.A. (2002). U–Pb zircon dating and Sr isotope systematics of the Vindhyan Supergroup India. Geology, vol. 30, pp. 131-134.

Romanovski, S.I. (1977). Sedimentologicheskie osnovy litologii [Sedimentological fundamentals of lithology] Nedra Leningrad 408p [in Russian].

Roy, A.B. (1988). Stratigraphic and tectonic framework of the Aravalli Mountain Range In Precambrian of the Aravalli Mountain Rajasthan India Mem. Geological Society of India, vol. 7, pp. 3-31.

Roy, A. B. and Kataria, P. (1999). Precambrian geology of the Aravalli Mountain and

neighbourhood: Analytical update of recent studies; Proc. Sem. Geology of Rajasthan: Status and Perspective, MLS University, Udaipur, pp.1-56.

Roy, A.B. and Kröner, A. (1996). Single zircon evaporation ages constraining the growth of the Archaean Aravalli craton northwestern Indian shield. Geological Magazine, vol. 133(3), pp. 333-342.

Roy, A.B. and Jakhar, S.R. (2002). Geology of Rajasthan (Northwest India) Precambrian to Recent; Scientific Publishers (India) Jodhpur, 421p.

Sinha Roy, S. (1984). Precambrian crustal interactions in Rajasthan NW India; Proceeding of Seminar on Crustal Evolution of Indian Shield and its Bearing on Metallogeny, pp. 84-91.

Sinha-Roy, S., Malhotra, G. and Mohanty, M. (1998). Geology of Rajasthan. Geol. Soc. India Bangalore 278p.

Sukanta, G., Atanu, M., Purnajit, B. and Syed, Z. (2017). Primary sedimentary structures and MISS in Gulcheru quartzite along SW part of Cuddapah Basin. Journal of the Geological Society of India, vol. 89, pp. 511-520.

Tanner, W.F. (1967). Ripple mark indices and their uses. Sedimentology, vol. 9, pp. 89-104.

Tanner, W.F. (1970). Triassic-Jurassic lakes in New Mexico. The Mountain Geologist.

Tanner, W.F. (1971). Numerical estimates of ancient waves water depth and fetch. Sedimentology, vol. 16, pp. 71-88.

Tanner, L.H. (1982). Description interpretation and geologic history of the Peru Sand outcrop in Catoosa Oklahoma, pp. 344-355.

Tricker, A.R. (1965). Bores Breakers Waves and Wakes; Elsevier New York NY 250 p.

Wang, W., Cawood, P.A., Pandit, M.K., Zhou, M.F. and Chen, W.T. (2017). Zircon U-Pb age and Hf isotope evidence for Eoarchean crustal remnant and crustal growth and reworking respond to supercontinental cycles in NW India. Journal of Geological Society, v. 174, pp. 759 -772.

Wiedenbeck, M., Goswami, J.N. and Roy, A.B. (1996). Stabilization of the Aravalli Craton of northwestern India at 2.5 Ga: an ion microprobe zircon study. Chemical Geology, v. 129 (3-4), pp. 325-340.

Received on: July 3, 2024
Revised accepted on: Sept 18, 2024